

Systematics of $\beta\beta$ decay sensitive medium mass nuclei using quadrupole-quadrupole plus pairing interactions

P. K. Raina

Department of Physics and Meteorology, Indian Institute of Technology, Kharagpur 721 302, India

S. K. Dhiman

Department of Physics, Himachal Pradesh University, Shimla 171 005, India

(Received 19 January 2000; revised manuscript received 5 September 2000; published 9 July 2001)

We present a microscopic variational model calculation to study the systematics of promising $\beta\beta$ decaying medium mass nuclei of ^{100}Mo , ^{104}Ru , ^{110}Pd , ^{114}Cd , ^{116}Cd , ^{124}Sn , ^{128}Te , and ^{130}Te along with their daughters. The calculations have been attempted in the s - d - g - h shell using the pairing plus quadrupole-quadrupole ($P + QQ$) interaction. This framework is found to be quite successful in describing the yrast 0^+ and 2^+ states of most of these nuclei when appropriate changes in the neutron-proton interaction component are taken into account. We also present 2ν $\beta\beta$ decay half-lives for ^{100}Mo and ^{116}Cd .

DOI: 10.1103/PhysRevC.64.024310

PACS number(s): 21.60.-n, 21.30.-x, 21.10.Ky, 23.40.Hc

Nuclear structure studies have recently acquired some special importance, apart from other reasons, due to the strong theoretical as well as experimental interest [1–11] in the problem of $\beta\beta$ decay. The neutrinoless decay mode plays a unique role [1–6] in investigating the basic nature of the neutrino. In this context, there are many open questions from the nuclear structure point of view. The most important is the reliability of the models and their ingredients. Specifically, the choice of the effective two-body interaction for the calculation of the double-beta ($\beta\beta$) decay nuclear matrix elements is crucial.

The mass region $A = 100$ has been of considerable interest for nuclear structure studies [12,13] as it shows the interplay of many interesting features. These nuclei have been found to display backbending at high spins and shape transitions [12]. Many attempts have been made in the past to explore these structural changes. The gradual structural changes in this region have been attributed to the exceptional strength of n - p interactions [14]. Inelastic electron scattering studies have acted as a very sensitive probe for dynamic changes in nuclei at the microscopic level [15]. This has been demonstrated through transition charge density studies for Pd and Cd nuclei [16,17]. These studies lead to a clear discrimination of the isoscalar (through the neutron-proton) and isovector (through the proton-proton and neutron-neutron) parts of the interaction. It has been shown explicitly that n - p interaction strengths have a deformation producing tendency.

For more than a decade, this region has also become interesting from the point of view of sensitivity to $\beta\beta$ decay as most of the potential nuclei fall within it. $\beta\beta$ decay half-life measurements for many of these nuclei have been done for ground state (g.s.) to g.s. transitions with a high level of confidence, and attempts are being made for others. In the case of nuclei like ^{100}Mo and ^{116}Cd , the transition rates to excited states of the daughter nuclei have also been measured experimentally [7,9]. Theoretical results [2–6,18,19] for the $\beta\beta$ decay nuclear matrix elements and half-lives for transitions from the g.s. of the initial nucleus to the g.s. and 2^+ state of the final nucleus have also been reported in different versions of the quasirandom phase approximation (QRPA).

Still, a systematic and more reliable theoretical study in this region is lacking. Here we do not go into a detailed investigation of the models being currently used but focus our attention on the effective interaction aspect only.

In order to develop understanding of two-body effective interaction changes while moving toward the drip line, recently, shell model studies have been undertaken [20] for some f - p shell nuclei using a modified KB realistic interaction. This shell has the advantage that the best possible comparison [21] among different nuclear microscopic models (especially with the recent large scale shell model) along with different tested effective interactions is possible. A remarkable observation about the success of extended pairing plus quadrupole-quadrupole ($P + QQ$) interaction has been made in a series of very recent papers [21–24]. It is shown that $P + QQ$ interaction gets very close to the realistic effective interaction with the singlet part of the interaction playing a very sensitive role.

It was observed [18,19] that, independent of the model used, the effective two-body interactions play a crucial role in the calculation of $\beta\beta$ decay nuclear matrix elements. In fact, the role of two-body effective interactions can be divided into two parts; one associated with the pairing interaction aspect and another taking care of deformation. In the mass region $A = 100$ the strong dependence of nuclear properties on the neutron-proton component of the QQ interaction, augmented by the success of the extended $P + QQ$ interaction in the f - p region, has motivated us to look into a study of systematics of $\beta\beta$ decay sensitive nuclei in the mass $A = 100$ –130 region with $P + QQ$ interactions.

A theoretical study of the electromagnetic properties for a large number of nuclei, and their comparison with experimental results, provides a broader base for testing the interaction and the model. Detailed studies of $\beta\beta$ decay nuclear matrix elements have also been taken up by us and preliminary investigations are showing encouraging results. To have an idea about the 2ν $\beta\beta$ decay half-lives that we get with this interaction, their values for ^{100}Mo and ^{116}Cd nuclei are given at the end of this paper. Now we provide a brief outline of the theoretical framework used in the present calculations

and then compare our results with available experimental data.

The ground and excited states of the even-even nuclei involved in the $\beta\beta$ decay transition are generated within Hartree-Fock-Bogoliubov theory in conjunction with the variation after angular momentum projection technique (hereafter denoted by VAP-HFB). The procedure adopted to calculate the axially symmetric wave function for the intrinsic state is the same as used in Ref. [16]. The expression for the matrix elements of the quadrupole operator between the different intrinsic states is

$$\begin{aligned} & \langle \Psi_K^{J'}(\beta) | Q_0^2 | \Psi_K^J(\beta) \rangle \\ &= \sqrt{\frac{1}{2}} [n^J(\beta) n^{J'}(\beta)]^{-1/2} \frac{1}{2} (2J+1) \\ & \times \int_0^{\pi/2} \sum_{\mu} \begin{bmatrix} J & 2 & J' \\ -\mu & \mu & 0 \end{bmatrix} d_{\mu 0}^J(\theta) n(\beta', \beta, \theta) \\ & \times \left[b^2 \sum_{\tau_3 \alpha \beta} e_{\tau_3} \langle \alpha | Q_{\mu}^2 | \beta \rangle \rho_{\alpha \beta}^{\tau_3}(\beta', \beta, \theta) \right] \sin \theta d\theta, \end{aligned}$$

where

$$n^J(\beta) = \int_0^{\pi} \{ \det[1 + F(\beta, \theta) f^{\dagger}(\beta)] \}^{1/2} d_{00}^J(\theta) \sin \theta d\theta,$$

$$n(\beta, \beta', \theta) = \{ \det[1 + F(\beta, \theta) f^{\dagger}(\beta')] \}^{1/2}.$$

The density matrices are given by

$$\rho_{\alpha \beta}^{\tau_3}(\beta, \beta', \theta) = \left[\frac{M(\beta, \beta', \theta)}{1 + M(\beta, \beta', \theta)} \right].$$

Here

$$M(\beta, \beta', \theta) = F(\beta, \theta) f^{\dagger}(\beta').$$

Reduced electric quadrupole transition rates and electric quadrupole moments are computed from

$$B(E2; 0^+ \rightarrow 2^+) = \frac{1}{16\pi} |\langle \Psi_0^2 | Q^2 | \Psi_0^2 \rangle|^2 \quad \text{and}$$

$$Q(2^+) = \langle \Psi_{22}^2 | Q_0^2 | \Psi_{22}^2 \rangle$$

with

$$Q_{\mu}^2 = \sqrt{\frac{16}{3}} \pi (r^2/b^2) Y_{\mu}^2(\Omega),$$

where b is the oscillator length parameter.

The matrices $f(\beta, \theta)$ and $F(\beta, \theta)$ are built from the coefficients $C_{j\alpha i}^{m\alpha}$, the expansion coefficients computed from the Hartree-Fock solutions, and $U_i^{m\alpha}$ and $V_i^{m\alpha}$, the pairing probabilities computed from BCS equations. These matrices carry the information about two-body and pairing interactions among the proton-proton, neutron-neutron, and proton-neutron pairs.

In the present calculations we treat the doubly closed shell nucleus ^{76}Sr as an inert core and the valence space is spanned by $1p_{1/2}$, $0g_{9/2}$, $1f_{5/2}$, $2s_{1/2}$, $1d_{3/2}$, $0g_{7/2}$, and $0h_{11/2}$ proton and neutron orbits. The set of single particle energies used here, given (in MeV) by $\epsilon(1p_{1/2}) = -0.8$, $\epsilon(0g_{9/2}) = 0.0$, $\epsilon(1d_{5/2}) = 5.4$, $\epsilon(2s_{1/2}) = 6.4$, $\epsilon(1d_{3/2}) = 7.9$, $\epsilon(0g_{7/2}) = 8.4$, and $\epsilon(0h_{11/2}) = 8.8$, has been employed in a number of successful shell model as well as variational model calculations of nuclear properties in the $A = 100$ mass region [25–29].

The pairing part of the $P + QQ$ effective interaction can be defined by the equation

$$V_P = -\frac{G}{4} \sum_{m, m'} S_m S_{m'} a_m^{\dagger} a_m^{\dagger} a_m a_{m'}.$$

m' corresponds to the time reversed state of m , G is the pairing interaction strength, and S_m is the phase factor $(-1)^{l-1}$. The strength of pairing forces is fixed through the approximate relation $G = -18$ MeV/A. The quadrupole-quadrupole part of the effective interaction is given by

$$\begin{aligned} V_{Q-Q} &= -(\chi/2) \sum_{mm', nn'} \langle m | q_{\mu}^2 | n \rangle \langle m' | q_{\mu}^2 | n' \rangle \\ & \times (-1)^{\mu} a_m^{\dagger} a_m^{\dagger} a_n a_{n'}. \end{aligned}$$

Here q_{μ}^2 is the quadrupole operator and χ is the $Q-Q$ strength parameter.

We know that the spin-isospin correlations are very important in weak interaction studies and here these correlations are reflected through χ . The strength of the χ has been fixed [16,17,25] through very sensitive electromagnetic probes (transition densities) for many of the systems under study. Its values for the proton-proton and neutron-neutron components (both corresponding to the triplet isospin channel) are taken as $\chi_{\pi\pi} = (\chi_{\nu\nu}) = -0.0105$ MeV b^{-4} for all nuclei involved in $\beta\beta$ decay processes. The magnitude of the strength parameter for the proton-neutron component (which corresponds to the singlet isospin channel) is taken as $\chi_{\pi,\nu} = -0.0265$ MeV b^{-4} for Mo and Ru nuclei, $\chi_{\pi,\nu} = -0.023$ MeV b^{-4} for Pd, $\chi_{\pi,\nu} = -0.020$ MeV b^{-4} for Cd, and $\chi_{\pi,\nu} = -0.0300$ MeV b^{-4} for Sn and Te nuclei. Here b is the oscillator parameter. These values for the strengths of the $Q \cdot Q$ interaction parameters are comparable to those suggested by Arima [26].

The results for the energy spectra are given in Fig. 1 and the reduced electric quadrupole transition rates $B(E2; 0_1^+ \rightarrow 2_1^+)$ along with the electric quadrupole moments $Q(2_1^+)$ are presented in Table I.

Yrast spectra. The energy spectra of ^{100}Mo , ^{100}Ru , ^{110}Pd , $^{110,114,116}\text{Cd}$, $^{114,116}\text{Sn}$, $^{128,130}\text{Te}$, and $^{128,130}\text{Xe}$ nuclei in Fig. 1 show that the theoretical results compare well with experimental ones for ^{100}Mo , ^{100}Ru , ^{110}Pd , and ^{110}Cd nuclei. The calculation is seen to reproduce the observed energy levels with $J^{\pi} \leq 6^+$. In the case of ^{110}Pd and ^{110}Cd nuclei, $J^{\pi} = 8^+$ and 6^+ , respectively, are also reproduced with good accuracy. The results for ^{110}Cd have also been compared with a recently observed energy level scheme of the ^{110}Cd

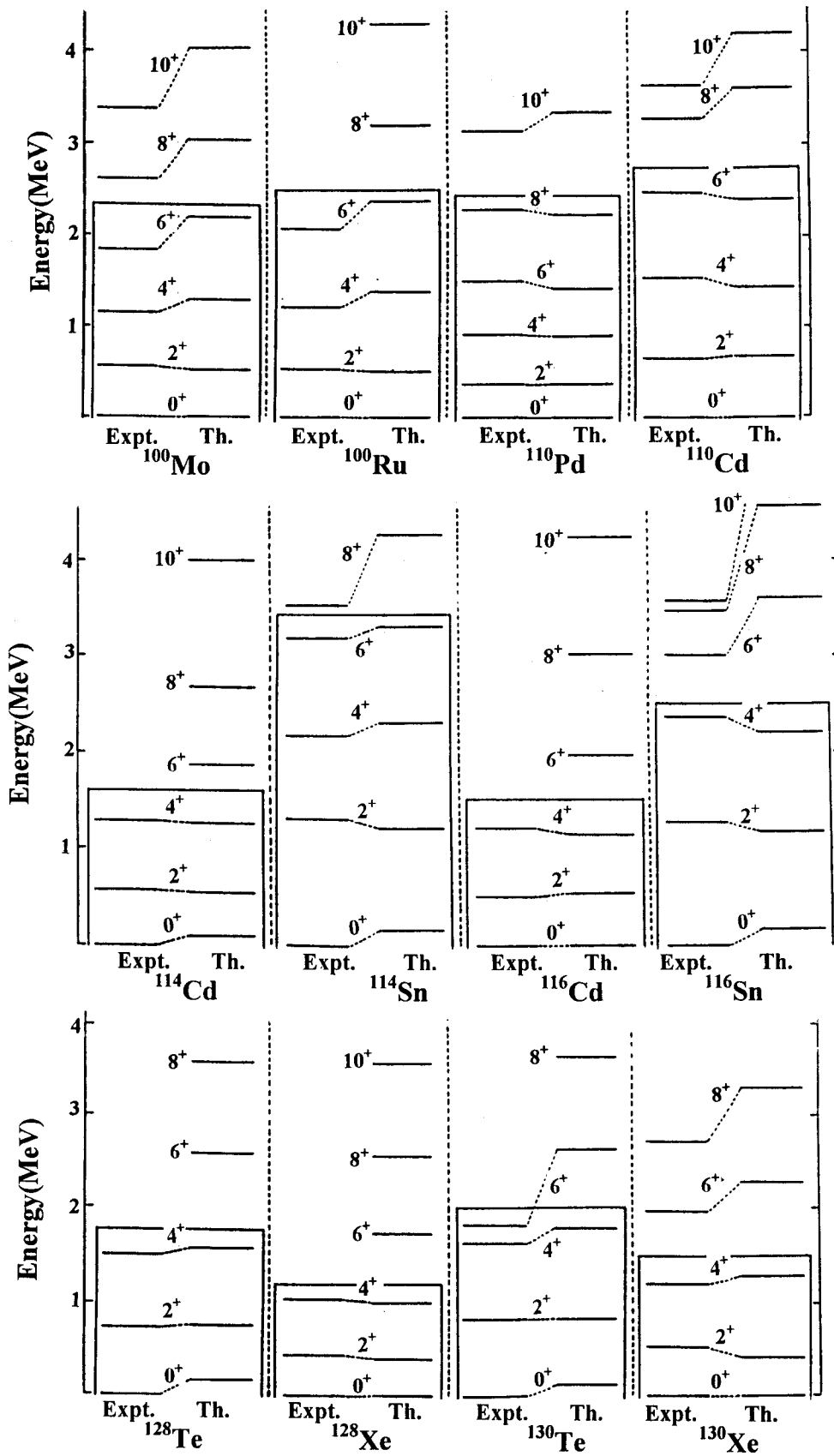


FIG. 1. Comparison of observed and calculated yrast spectra for ^{100}Mo , ^{100}Ru , ^{110}Pd , $^{110,114,116}\text{Cd}$, $^{114,116}\text{Sn}$, $^{128,130}\text{Te}$, and $^{128,130}\text{Xe}$ nuclei.

TABLE I. Comparison of computed and observed transition probabilities $B(E2;0^+ \rightarrow 2^+)$ and quadrupole moments $Q(2)$ for some even-even nuclei in the mass 100–130 region. Effective charges are $e_x = 1 + e_\nu$ and $e_\nu = e_{\text{eff}}$.

Nucleus	$B(E2;0^+ \rightarrow 2^+) \times 10^{-50} e^2 \text{cm}^4$			$Q(2^+) \times 10^{-24} \text{cm}^2$				
	Expt. ^a	Theory		Expt. ^b	Theory			
		e_{eff}			e_{eff}			
		0.2	0.3	0.4	0.1	0.2	0.3	
¹⁰⁰ Mo	51.6±0.10	42.53	49.72	58.21	-0.42±0.09	-0.34	-0.39	-0.42
¹⁰⁰ Ru	50.1±0.10	43.09	51.20	57.75	-0.43±0.07	-0.36	-0.42	-0.47
¹⁰⁴ Ru	84.1±0.16	72.95	83.39	90.62		-0.29	-0.35	-0.38
¹⁰⁴ Pd	53.5±0.35	45.00	55.78	68.3	-0.47±0.10	-0.45	-0.48	-0.52
¹¹⁰ Pd	87.0±0.40	75.72	88.10	94.57	-0.55±0.08	-0.51	-0.59	-0.65
¹¹⁰ Cd	45.0±0.20	44.23	47.36	51.06	-0.40±0.04	-0.29	-0.34	-0.41
¹¹⁴ Cd	55.0±0.20	53.07	59.00	62.54	-0.35±0.12	-0.32	-0.35	-0.39
¹¹⁴ Sn	23.5±0.50	18.42	20.49	24.58	-0.36	-0.33	-0.37	-0.38
¹¹⁶ Cd	56.0±0.20	44.63	55.76	61.08	-0.42±0.08	-0.35	-0.42	-0.44
¹¹⁶ Sn	20.9±0.60	19.29	21.05	25.09	-0.17±0.04	-0.12	-0.13	-0.16
¹²⁴ Sn	16.6±0.40	10.47	14.53	17.40	-0.01±0.17	-0.24	-0.26	-0.29
¹²⁴ Te	61.0±0.20	62.05	64.81	67.57	-0.45±0.06	-0.34	-0.37	-0.42
¹²⁸ Te	38.3±0.06	30.67	34.56	38.92	-0.14±0.12	-0.20	-0.23	-0.25
¹²⁸ Xe	75.0±0.40	69.12	74.42	78.45		-0.12	-0.15	-0.25
¹³⁰ Te	29.5±0.07	21.05	25.81	29.10	-0.15±0.10	-0.19	-0.23	-0.25
¹³⁰ Xe	65.0±0.05	64.47	68.72	72.02		-0.17	-0.18	-0.23

^aReference [32].

^bReference [33].

nucleus obtained from the ¹¹⁰In^m β decay [31]. The yrast spectra for the nuclei ¹⁰⁰Mo and ¹⁰⁰Ru are almost rotational with $(E_2 - E_0) \approx 0.5$ MeV and the VAP-HFB results for $J^\pi = 0^+$ and 2^+ are in excellent agreement with experiments. But for $J^\pi = 6^+$ and beyond the levels in Mo and Ru nuclei show some discrepancy, possibly because of some dynamical changes at high spin. However, we are presently concerned with low J value states.

It is difficult to reproduce the energy spectrum for Sn isotopes. Figure 1 shows that ¹¹⁴Sn and ¹¹⁶Sn are not rotational nuclei and hence there is discrepancy for these isotopes with the observed yrast spectra. In the case of ¹¹⁴Cd and ¹¹⁶Cd, the VAP-HFB theory works well in reproducing observed yrast levels, especially for ¹¹⁶Cd. The comparisons for ^{128,130}Te and ^{128,130}Xe nuclei show that the calculations are able to reproduce the observed levels with $J^\pi \leq 4^+$ within a fair amount of accuracy. In the case of ¹¹⁴Cd, Sn, and Te nuclei the calculated $J^\pi = 2^+$ levels matched the observed values.

Reduced electric quadrupole transition rates and electric quadrupole moments. We next consider the reduced transition probabilities $B(E2;0_1^+ \rightarrow 2_1^+)$ and electric quadrupole moments $Q(2)$ in the case of ¹⁰⁰Mo, ^{100,104}Ru, ^{104,110}Pd, ^{110,114,116}Cd, ^{114,116,124}Sn, ^{124,128,130}Te, and ^{128,130}Xe nuclei. In Table I we present the experimental results along with our computed $B(E2)$ values. It is seen that the present microscopic description permits an adequate interpretation of data for the available electromagnetic properties in terms of a reasonable variation of the isoscalar effective charges. The

computed $B(E2)$ and $Q(2)$ estimates are in good agreement with the experiments for e_{eff} variation within 0.20 to 0.40. Mo, Ru, Pd, and Cd nuclei are in excellent agreement and have a consistent value around $e_{\text{eff}} = 0.30$. Exceptions are for $Q(2)$ values in the case of ¹¹⁶Sn and ¹²⁴Te nuclei. Experimental errors are too large for ^{128,130}Te to make any comparison. $B(E2)$ values are not reproduced in the case of Te nuclei within the chosen range of e_{eff} .

2 $\nu\beta\beta$ decay half-lives for ¹⁰⁰Mo and ¹¹⁶Cd. Experimental and theoretical results for $2\nu\beta\beta$ decay half-lives of ¹⁰⁰Mo and ¹¹⁶Cd nuclei are presented in Table II. We observe that the second QRPA (SRPA) description, obtained by removing the discrepancies of the empirical QRPA (EQRPA), provides results closer to experimental values. There has been an attempt in the case of ¹⁰⁰Mo within the pseudo-SU(3) scheme, for both axially deformed (def) and spherically limiting (sph) cases, where the decay rates are found to be strongly dependent on proton and neutron occupation numbers. In the case of the ¹¹⁶Cd nucleus, SRPA with Woods-Saxon (WS) and QRPA with adjusted Woods-Saxon (AWS) results are also shown.

We note that our results are better than most versions of the QRPA. The SRPA result, which is closer to the experimental value in the case of ¹⁰⁰Mo, fails for ¹¹⁶Cd. The HFB results show more consistency. Of considerable interest is the case of ¹⁰⁰Mo where our result is closer to the successful one coming from the SU(3) deformed model. This clearly indicates that the role of deformations is important in this region. The finer details of the quantitative aspects of the role of

TABLE II. Half-lives for $2\nu\beta\beta$ decay in the case of ^{100}Mo and ^{116}Cd . Experimental values along with available theoretical values (taken from [30]) are also presented for comparison.

Nucleus	Experimental half-lives (10^{19} yr)	Theoretical values of half-lives in different models (10^{19} yr)				
		EQRPA	SRPA	SU(3) sph	SU(3) def	Present
^{100}Mo	0.95	0.29	3.2	0.49	0.96	1.14
^{116}Cd	3.75	QRPA+AWS		SRPA+WS	Present	
		5.1		10.0	1.2	

deformation are under study. Once a proper understanding of the role of deformation is obtained in more detail and the effects are studied on $0\nu\beta\beta$ decay matrix elements, we expect to bring out results with good predictive power in the case of other $\beta\beta$ decay nuclei in this region that have yet to be brought to a good confidence level. The nuclear matrix element evaluation has to be brought onto a better footing before we compute weak interaction parameters and the effective neutrino mass.

The present work makes use of the pairing plus quadrupole-quadrupole effective interaction for the calculations of spectra, quadrupole transition probabilities, and static moments for $\beta\beta$ sensitive medium mass nuclei. Different n - p interaction strength parameters, fixed through studies of sensitive electromagnetic properties like transition charge densities, have been used for different sets of nuclei. The

motivation for such studies has been provided by the recent observation of the closeness of the $P+QQ$ interaction to the realistic interaction if the n - p component is taken into account carefully. The self-consistent HFB solutions provide encouraging results for the first few excited states with excellent matching for Mo, Ru, Cd, and Pd nuclei. The HFB results for the half-lives of ^{100}Mo and ^{116}Cd , the best known $2\nu\beta\beta$ decay cases in the medium mass region, are also encouraging. The role of deformations appears to be important and the HFB method is the best choice to handle this effect. In particular, ^{100}Mo can be used as a base candidate for exploring the finer effects of deformation on nuclear matrix elements. Once the effect of deformations on nuclear matrix elements is clearly identified, calculations for other cases as well as the 0ν mode will be more reliable and hence have better predictive power.

- [1] W. C. Haxton and G. J. Stephenson, Jr., *Prog. Part. Nucl. Phys.* **12**, 409 (1984).
- [2] M. Doi, T. Kotani, and E. Takasugi, *Prog. Theor. Phys. Suppl.* **83**, 1 (1985).
- [3] T. Tomoda, *Rep. Prog. Phys.* **54**, 53 (1991).
- [4] M. Moe and P. Vogel, *Annu. Rev. Nucl. Part. Sci.* **44**, 274 (1994).
- [5] A. Faessler and F. Simcovic, hep-ph/9901215; *J. Phys. G* **24**, 2139 (1998).
- [6] H. V. Klapdor-Kleingrothaus, hep-ex/9802007; hep-ex/9901021; *Int. J. Mod. Phys. A* **13**, 3953 (1998).
- [7] A. Morales, *Nucl. Phys. B (Proc. Suppl.)* **77**, 335 (1999).
- [8] H. Ejiri, *Nucl. Phys. B (Proc. Suppl.)* **77**, 345 (1999).
- [9] F. A. Danevich *et al.*, *Phys. Lett. B* **344**, 72 (1995).
- [10] J. Toivanen and J. Suhonen, *Phys. Rev. Lett.* **75**, 410 (1995).
- [11] C. Barbero, F. Krmpotic, and A. Mariano, *Phys. Lett. B* **436**, 49 (1998); **345**, 192 (1995).
- [12] E. Cheifetz, R. C. Jared, S. G. Thomson, and J. B. Wilhelm, *Phys. Rev. Lett.* **25**, 38 (1970); D. Hook *et al.*, *J. Phys. G* **12**, 1277 (1986).
- [13] S. Pittel, *Nucl. Phys.* **A347**, 417 (1980).
- [14] J. Eberth, R. A. Meyer, and K. Sistemich, *Proceedings of the International Workshop on Nuclear Structure in the Zirconium Region*, Bad Honnef, 1988 (Springer, Berlin, 1988).
- [15] J. Heisenberg and H. P. Bloch, *Annu. Rev. Nucl. Part. Sci.* **33**, 569 (1983).
- [16] A. J. Singh, P. K. Raina, and S. K. Dhiman, *Phys. Rev. C* **50**, 2307 (1994).
- [17] A. J. Singh and P. K. Raina, *Phys. Rev. C* **52**, R2342 (1995).
- [18] G. Pantis, F. Simcovic, J. D. Vergados, and Amand Faessler, *Phys. Rev. C* **53**, 695 (1996).
- [19] J. Engel, P. Vogel, and M. R. Zirnbauer, *Phys. Rev. C* **37**, 731 (1988).
- [20] E. Caurier, G. Martinez-Pinedo, F. Nowacki, A. Poves, J. Retamosa, and A. P. Zuker, *Phys. Rev. C* **59**, 2033 (1999).
- [21] M. Hasegawa, K. Kaneko, and S. Tazaki, nucl-th/9910068.
- [22] K. Hara, Y. Sun, and T. Mizusaki, *Phys. Rev. Lett.* **83**, 1922 (1999).
- [23] M. Hasegawa and K. Kaneko, *Phys. Rev. C* **59**, 1449 (1999).
- [24] M. K. Kaneko and M. Hasegawa, *Phys. Rev. C* **60**, 024301 (1999).
- [25] A. J. Singh and P. K. Raina, *Phys. Rev. C* **53**, 1258 (1996).
- [26] A. Arima, *Nucl. Phys.* **A354**, 19 (1981); A. Arima and G. Gillet, *Ann. Phys. (N.Y.)* **66**, 117 (1971); A. Arima, T. Otsuka, F. Iachello, and I. Talmi, *Phys. Lett.* **66B**, 205 (1977).
- [27] E. Moya de Guerra, P. Sarriguren, and L. Zamick, *Phys. Rev. C* **56**, 863 (1997).
- [28] P. Federman and S. Pittel, *Phys. Lett.* **77B**, 29 (1978); E. Krichusc, P. Federman, and S. Pittel, *Phys. Rev. C* **47**, 567 (1993).
- [29] Arun Bharti and S. K. Khosa, *Nucl. Phys.* **A572**, 317 (1994); S. K. Sharma, P. N. Tripathi, and S. K. Khosa, *Phys. Rev. C* **38**, 2938 (1988).
- [30] J. Suhonen and O. Civitarese, *Phys. Rep.* **300**, 123 (1998).
- [31] M. Bertschy *et al.*, *Phys. Rev. C* **51**, 103 (1995).
- [32] S. Raman *et al.*, *At. Data Nucl. Data Tables* **36**, 1 (1987).
- [33] Promila Raghawan, *At. Data Nucl. Data Tables* **42**, 189 (1989).